Surv Geophys (2012) 33:733–744
DOI 10.1007/s10712-012-9187-x

Diagnosing Climate Feedbacks in Coupled Ocean–Atmosphere Models

Eui-Seok Chung · Brian J. Soden · Amy C. Clement

Received: 22 November 2011 / Accepted: 21 February 2012 / Published online: 15 March 2012

Abstract We review the methodologies used to quantify climate feedbacks in coupled models. The method of radiative kernels is outlined and used to illustrate the dependence of lapse rate, water vapor, surface albedo, and cloud feedbacks on (1) the length of the time average used to define two projected climate states and (2) the time separation between the two climate states. Except for the shortwave component of water vapor feedback, all feedback processes exhibit significant high-frequency variations and intermodel variability of feedback strengths for sub-decadal time averages. It is also found that the uncertainty of lapse rate, water vapor, and cloud feedback decreases with the increase in the time separation. The results suggest that one can substantially reduce the uncertainty of cloud and other feedbacks with the accumulation of accurate, long-term records of satellite observations; however, several decades may be required.

Keywords Climate feedbacks · Kernels · Time dependence

1 Background

Climate models employed to predict future climate in response to the projected increase in anthropogenic greenhouse gases exhibit substantial intermodel variations. Considering that the response of climate system to a given radiative forcing is determined by a number of feedback processes that amplify or dampen the initial radiative perturbation, the intermodel spread is attributed to the differences in climate feedbacks depicted in climate models and thus requires better understanding of climate feedbacks in order to reduce the uncertainty in climate sensitivity.

Climate feedbacks have been quantified by a number of different approaches. At first, offline processing approaches have been applied to CO_2 doubling experiments of climate models with mixed-layer oceans. Hansen et al. (1984) conducted feedback calculations for water vapor, snow/ice albedo, and clouds based on one-dimensional radiative convective

E.-S. Chung (✉) · B. J. Soden · A. C. Clement
Rosenstiel School of Marine and Atmospheric Science, University of Miami, Miami, FL, USA
e-mail: e.chung@miami.edu

model (RCM) and suggested that cloud feedback amplifies global warming. However, it was pointed out that spatiotemporal averages of nonlinear variables required for RCM methods may cause uncertainties in global feedback values (e.g., Wetherald and Manabe 1988). By contrast, Wetherald and Manabe (1988) introduced an offline partial radiative perturbation (PRP) method in which the change in top-of-atmosphere (TOA) radiative fluxes is computed by substituting one variable at a time from the perturbed climate state into the control climate. This method can be complicated and computationally expensive due to repeated offline three-dimensional radiative transfer calculations. Colman (2003) intercompared the published strengths for water vapor, lapse rate, surface albedo, and cloud feedbacks determined from the offline PRP methods for CO_2 doubling experiments and showed that the intermodel differences are substantial for all climate feedbacks. However, Colman (2003) emphasized that the substantial intermodel differences could be caused by the absence of a consistent comparison methodology.

The CO_2 doubling experiments require substantial amounts of computer time for the ocean to equilibrate, and differences in control climates could cause spurious differences in climate sensitivity between climate models (e.g., Cess et al. 1990). In order to avoid such difficulties, uniform perturbations in sea surface temperature were prescribed for a fixed season to induce a change in TOA radiative fluxes, and the resulting changes in clear-sky fluxes and cloud radiative forcing were used to infer clear-sky sensitivity and cloud feedback (Cess et al. 1990). Although this approach is much simpler compared to the offline approaches, uniform perturbations in sea surface temperature for a fixed season may not represent realistic climate change conditions (e.g., Colman 2003; Soden and Held 2006). In addition, feedbacks other than clouds cannot be quantified from this approach. Furthermore, it was pointed out that non-cloud feedbacks can be included in the cloud-forcing term (e.g., Zhang et al. 1994; Colman 2003; Soden et al. 2004; Soden and Held 2006).

A radiative kernel approach was proposed as an alternative method to facilitate the analysis of climate feedbacks (Soden and Held 2006; Soden et al. 2008; Shell et al. 2008). Radiative kernels describe the differential response of TOA radiative fluxes to incremental changes in the feedback variables. The use of radiative kernels enables one to decompose a feedback into two parts: one that depends on radiative transfer and the unperturbed climate state, and a second factor that arises from the climate response of the feedback variable. This approach avoids the effects of field decorrelation which introduce substantial biases in traditional feedback analyses that assume all feedback variables to be temporally uncorrelated (Colman 2003; Colman and McAvaney 2009). Furthermore, the kernel technique requires far fewer computations and is easier to implement than the traditional offline PRP methods (e.g., Wetherald and Manabe 1988). Thus, this approach facilitates an understanding of the causes and implications of differences among models, or between models and observations. The radiative kernel method showed that previous surveys of climate feedbacks exaggerated the intermodel differences in water vapor, lapse rate, and surface albedo feedbacks due to inconsistent methodology and that cloud feedback ranges from nearly neutral to positive in all climate models (Soden and Held 2006; Soden et al. 2008). In addition, the robustness of water vapor feedback was confirmed through the radiative kernel approach (John and Soden 2007).

Feedback processes affect internal variations (i.e., seasonal to decadal time scales) in surface temperature as well as externally forced changes, implying that the calculation of climate feedbacks between two climate states involves a combination of both internally and externally driven responses. Unfortunately, the length of satellite observations is not long enough to examine the time dependence of climate feedbacks (e.g., Dessler et al.

2008; Murphy et al. 2009; Chung et al. 2010a, b; Dessler 2010). Furthermore, the impact of internal variability on the climate feedbacks has not been fully investigated even in the cases of climate model simulations. Thus, it is important to gain insight on the time scales of climate feedbacks and the implications for detecting them from satellite observations. In doing so, the time dependence of feedback processes is examined using climate model simulations of the Intergovernmental Panel on Climate Change (IPCC) Fourth Assessment Report (AR4).

2 Data and Methodology

Climate change simulations for the IPCC AR4 Special Report on Emissions Scenarios (SRES) A1B scenario, which approximately corresponds to a doubling of carbon dioxide concentration between 2000 and 2100, are used to quantify the strength of feedbacks for temperature, water vapor, surface albedo, and clouds for 15 coupled ocean–atmosphere models (CCCMA CGCM3.1, CCCMA CGCM3.1-T63, CNRM CM3, CSIRO MK3.0, GFDL CM2.0, GFDL CM2.1, GISS ER, IAP FGOALS1.0.G, INMCM3.0, IPSL CM4, MIROC3.2-MEDRES, MPI ECHAM5, NCAR CCSM3.0, NCAR PCM1, and UKMO HADGEM1).

The feedback strength (λ_x) for variable x is computed following Soden and Held (2006), that is,

$$\lambda_x = (\partial R/\partial x)\left(\mathrm{d}x/\mathrm{d}\overline{T_s}\right)$$

where R and T_s denote the top-of-atmosphere net incoming radiative flux and surface temperature, respectively, and the overbar indicates the global averaging. The first term of λ_x, which depends on the radiative transfer and the unperturbed climate state, has been calculated by Soden et al. (2008) for temperature, water vapor (shortwave and longwave, separately), and surface albedo. We employed their values (termed radiative kernel) given as functions of latitude, longitude, altitude, and monthly resolved season. The second term represents the model response for each variable x and can be computed from model outputs by dividing the difference of variable x between two climate states A and B by the change of global mean surface temperature, that is, $\mathrm{d}x/\mathrm{d}\overline{T_s} = (x^B - x^A)/(\overline{T_s}^B - \overline{T_s}^A)$. The product of the model-computed climatic responses for each variable x with the radiative kernel corresponding to latitude, longitude, altitude, and month is vertically integrated from the surface to the tropopause. Then, we average the vertically integrated feedback parameter over the entire globe to provide global-average estimates of each feedback parameter.

It is noted that the temperature feedback is further subdivided into the response that results from a uniform temperature change throughout the troposphere (Planck feedback) and the modification due to the variation of atmospheric temperature profile (lapse rate feedback). Meanwhile, because of cloud masking effects (Zhang et al. 1994; Colman 2003; Soden et al. 2004, 2008; Soden and Held 2006), cloud feedback is computed by adjusting model-simulated change in cloud radiative forcing between two climate states following Soden et al. (2008).

The magnitude of climate feedbacks can also be estimated from short-term climate fluctuations such as ENSO or volcanic eruptions by regressing changes in the radiative fluxes at the top-of-atmosphere with surface temperature changes (e.g., Dessler and Wong 2009; Dessler 2010). However, the characteristics of radiative forcings associated with short-term climate fluctuations and resultant meridional pattern of surface temperature

changes are different from those corresponding to changes in greenhouse gas concentrations. As a result, it is unlikely that climate feedbacks estimated from short-term climate variations are directly comparable to climate feedbacks due to changes in greenhouse gases.

The subsequent sections examine the variations of each feedback parameter as a function of (1) the length of time average of the climate states A and B and (2) the time separation between climate states used to compute climate feedbacks. Both factors are critical for the design of observational systems intended to reduce uncertainties in climate feedbacks and climate sensitivity (National Research Council 2007).

3 Influences of the Length of Time Average to Define Climate States

Feedback strengths are computed for each model of the IPCC AR4 SRES A1B scenario by changing the length of climate states A and B, which ranges 1–20 years, with the fixed time separation between two climate states of 50 years. Considering the variation of feedback strengths in time (e.g., Murphy 1995; Senior and Mitchell 2000), feedback computations are repeated 50 times by moving the time location of climate states A and B by 1 year. Figures 1 and 2 display the computed feedback strengths as functions of time location as well as the length of time average used to define climate states. For example, the feedback strengths of year 2050 are derived by scaling the radiative kernels with the differences of projected climate of years (2050–2050) [(2050–2069)] from that of (2100–2100) [(2100–2119)] for the 1-year [20-year] time average case. In addition, standard deviation of a given feedback parameter is computed for each climate model, and the numeral in the upper-right corner of each panel denotes the average of the standard deviations of the individual models.

Figure 3 displays the average of the standard deviations of the individual models (closed circles) as a function of the length of the time average chosen for feedback computation, and the associated error bars (in blue) denote the range of standard deviations. Because the temperature increase is greater in the troposphere compared to the surface, mainly over the tropics, the reduction in lapse rate with the surface warming leads to an increase in the top-of-atmosphere outgoing longwave radiation (Fig. 1a) with a large intermodel variability due to a difference in the meridional patterns of surface warming (Soden and Held 2006). The magnitude of lapse rate feedback exhibits a smaller variation for the longer time average cases (Fig. 3a). Mean standard deviation decreases from 0.235 W m^{-2} K^{-1} (1-year case) to 0.071 W m^{-2} K^{-1} (20-year case) with a substantial reduction occurring for the shorter-term averaging cases ($\leq$5 years). Moreover, a couple of models produce even positive values for 1-year averaging case (Fig. 1a). Considering that the reduction in standard deviation and intermodel variability is not distinct for the averaging time scale longer than 10 years, a filtering of the sub-decadal timescale temperature fluctuations (primarily ENSO) is preferred to reduce the uncertainty in computed lapse rate feedback strengths. Although feedback strength is approximately constant (about -3.2 W m^{-2} K^{-1}) for Planck feedback, the year-to-year variation is not trivial for the shorter-term averaging cases (not shown).

The increase in water vapor with the surface warming results in a positive feedback with larger magnitudes for longwave spectrum regardless of the length of climate states (Fig. 1b, c). Although a couple of models show noticeable interannual variations in the case of the shortwave component, standard deviations and intermodel variability are quite small across different averaging timescales (Fig. 3b). On the other hand, the longwave

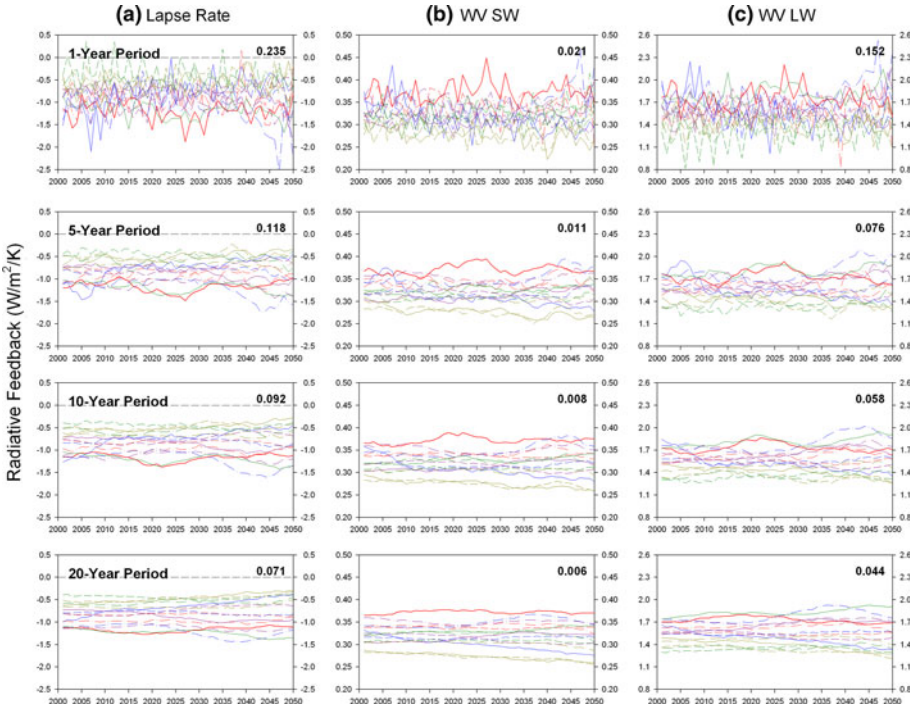

Fig. 1 Temporal variations of the feedback strengths computed from the IPCC AR4 SRES A1B simulations with the time separation between climate states A and B of 50 years: **a** lapse rate, **b** water vapor (shortwave), and **c** water vapor (longwave). The *numeral* in the *upper-right* corner of each panel denotes the average of the standard deviations of 15 climate models for a given feedback parameter and the length of time average used to define climate states

component of water vapor feedback exhibits distinctly larger temporal variations that are comparable to those of lapse rate feedback. Figure 3c shows the decrease of standard deviation from 0.152 W m^{-2} K^{-1} to 0.044 W m^{-2} K^{-1} with the increase in the length of time average from 1 to 20 years. Note that most of this decrease occurs for the sub-decadal time averages. Comparisons between lapse rate and water vapor feedbacks in Fig. 1 indicate that the larger feedback strength of water vapor feedback relative to lapse rate feedback renders the sum of these two feedbacks as being positive. In addition, the temporal variations are negatively correlated with each other, consistent with the strong coupling between the vertical structure of temperature and water vapor changes (e.g., Colman 2003; Allan 2006; Soden and Held 2006; John and Soden 2007; Soden et al. 2008; Colman and McAvaney 2009; Chung et al. 2010a). Therefore, the sum of lapse rate and water vapor feedbacks shows reduced temporal variations and intermodel variability, and less sensitivity to the length of the time average employed for feedback computations.

The lapse rate and water vapor feedbacks are augmented by the feedback process between surface temperature and surface albedo (Fig. 2a). In spite of a much smaller strength compared to lapse rate and water vapor feedbacks, the accuracy of computed surface albedo feedback is also influenced by the length of the time average of climate states (Fig. 3d). A large intermodel variability is likely to stem from differences in the

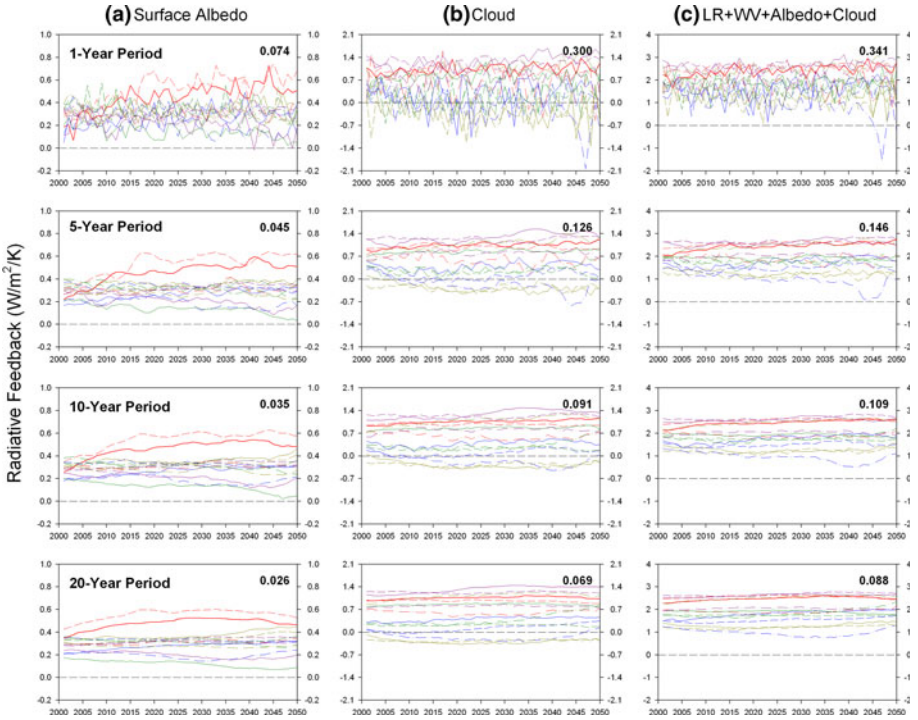

Fig. 2 Same as in Fig. 1, but for: **a** surface albedo, **b** cloud, and **c** summation except Planck feedback

depiction of snow/sea ice coverage changes and the meridional distributions of the changes (e.g., Colman and McAvaney 2009).

The cloud feedback was calculated from the change of the top-of-atmosphere net cloud radiative forcing and the difference between the all-sky and clear-sky radiative kernels following Soden et al. (2008). It is noted that changes in aerosol emission and thus aerosol indirect effect may affect the changes in cloud distribution in the model simulations of SRES A1B scenario. The temporal variations and intermodel differences are larger than any other feedback processes for all time averages (Fig. 2b). However, like other feedback processes, the use of longer time average reduces the uncertainty of inferred feedback strengths with an approximately exponential decrease for the sub-decadal time average cases (Fig. 3e). Given the offsetting influences between lapse rate and water vapor feedbacks arising from the strong coupling between the vertical structure of temperature and water vapor changes and smaller magnitude of surface albedo feedback, the uncertainty of combined feedback (Fig. 3f) is determined primarily by the cloud feedback (e.g., Colman 2003; Bony and Dufresne 2005; Bony et al. 2006; Soden et al. 2008; Colman and McAvaney 2009; Chung et al. 2010b; Dessler 2010).

Figure 3 also displays the dependence of the difference between the maximum and minimum value of the computed feedback strengths for a particular averaging interval with respect to the length of the time average used to define two climate states (open triangles). As shown in the cases of standard deviation, the ranges of computed feedback strengths manifest the influences of averaging time scale on lapse rate, water vapor (longwave component), and cloud feedbacks. Sub-decadal time average cases are characterized by

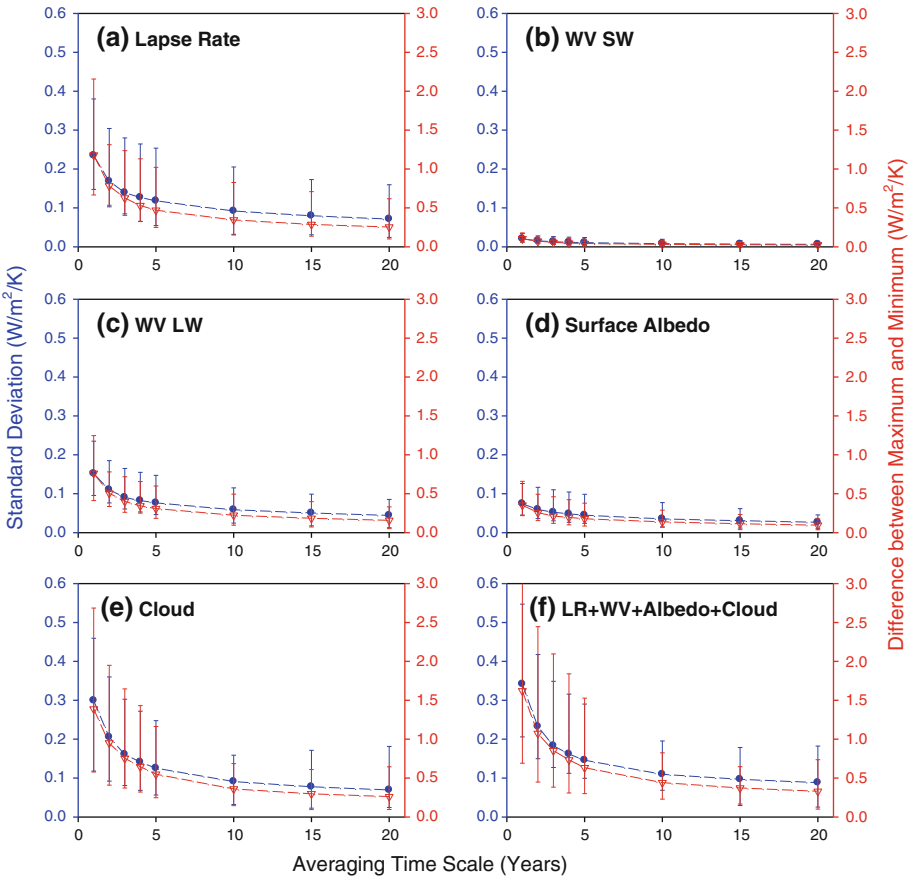

Fig. 3 Variations of standard deviation (*circles*) and the difference between the maximum and minimum value (*triangles*) of the feedback strengths computed, by setting the time separation between climate states A and B to 50 years, from the IPCC AR4 SRES A1B simulations as a function of the length of time average: **a** lapse rate, **b** water vapor (shortwave), **c** water vapor (longwave), **d** surface albedo, **e** cloud, and **f** summation except Planck feedback. *Symbols* (*circles* and *triangles*) and error bars denote the average and range of 15 climate models, respectively. Note that the axis and corresponding labels for the difference between the maximum and minimum value of the feedback strengths are placed on the right of the graphs

larger uncertainties due to smaller value of signal-to-noise ratio associated with seasonal to decadal scale natural variability. In addition, the intermodel variability denoted by the error bars (in red) decreases significantly with the increase in averaging time scale. Thus, the use of time average longer than sub-decadal time scale is required to filter high-frequency internal variations and thereby enhance the stability and robustness in the feedback computations.

Because of the difference in magnitude of each feedback process as shown in Figs. 1 and 2, the same value of standard deviation or the difference between the maximum and minimum could produce substantially different feedback uncertainty in terms of a percent error. Thus, the fractional differences are computed with respect to the feedback strengths of the 20-year averaging case (Table 1). All feedback processes produce the largest fractional difference for the 1-year averaging case, and the fractional differences reduce

Table 1 Fractional differences of feedback strengths relative to the values of 20-year averaging case

	Lapse rate	WV SW	WV LW	Albedo	Cloud	All
1-Year	19.3 ± 46.7	3.8 ± 11.0	4.4 ± 16.1	−5.8 ± 21.2	−64.0 ± 205.3	−18.7 ± 34.3
5-Year	18.2 ± 24.2	3.3 ± 3.8	4.2 ± 5.7	−10.8 ± 19.0	−15.6 ± 41.8	−6.7 ± 10.6
10-Year	7.3 ± 9.8	1.4 ± 1.4	1.8 ± 2.6	−4.9 ± 13.2	−11.7 ± 25.5	−1.6 ± 6.3
15-Year	4.8 ± 7.8	0.7 ± 0.9	1.0 ± 1.8	−2.4 ± 6.0	−2.8 ± 10.4	−0.2 ± 2.5

Numerals denote the average and standard deviation of 15 climate models. The unit is %

with the increase in averaging time scale. As expected, the largest percent error comes from cloud feedback, affecting the accuracy of the sum of all feedback processes. In addition, Table 1 exhibits that the fractional errors are larger for lapse rate and albedo feedback compared to both the components of water vapor feedback and that the strength of water vapor feedback can be confidently determined from even short-term observations (e.g., Allan 2006; John and Soden 2007; Dessler et al. 2008; Chung et al. 2010a).

4 Influences of the Time Separation of Two Climate States

With the operation of space-based hyper-spectral observations (e.g., AIRS and IASI), profiles of temperature and water vapor can be retrieved with sufficient vertical resolution to enable the computation of observational feedbacks using radiative kernels. While previous studies have estimated feedback strengths using those products (e.g., Dessler et al. 2008), short observational records (<10 years) have been an obstacle to investigating the time dependence of feedback parameters.

This limitation raises the following question. If one could perfectly measure temperature and humidity profiles and other climate variables from those satellite instruments, how many years of observations are required to determine climate feedbacks within a certain level of uncertainty? The problem is not strictly an observational one. The same question can be posed to the analysis of climate models, for example, How many years of model simulations are required to ensure the robustness of a model-diagnosed feedback strength? To address these questions, we examine the sensitivity of feedback parameters to the time separation between two climate states A and B.

Feedback computations are conducted with a time separation ranging from 20 to 50 years for three cases of time averaging (5, 10, and 20 years). For example, the feedback strengths of year 2001 for the 10-year averaging case are derived from the radiative kernels in conjunction with the differences of projected climate of years (2001–2010) from that of (2021–2030) [(2051–2060)] for the 20-year [50-year] time separation. Then, the temporal variations and intermodel variability of model-inferred feedback strengths are examined as in the previous section. On account of considerable high-frequency variations and intermodel discrepancies, the computation has not been conducted for the time averaging of 1–4 years. Figure 4 shows the average of the models' standard deviations of a given feedback parameter as a function of the time separation for three cases of time average length. All feedback processes manifest larger standard deviations for the shorter time average case, indicating that filtering of high-frequency internal fluctuations is required to reduce uncertainties in the feedback computations. The influence of the length of time average diminishes with the increase in the time separation between climate states A and B. This is a relevant consideration as a continuous record of high spectral resolution

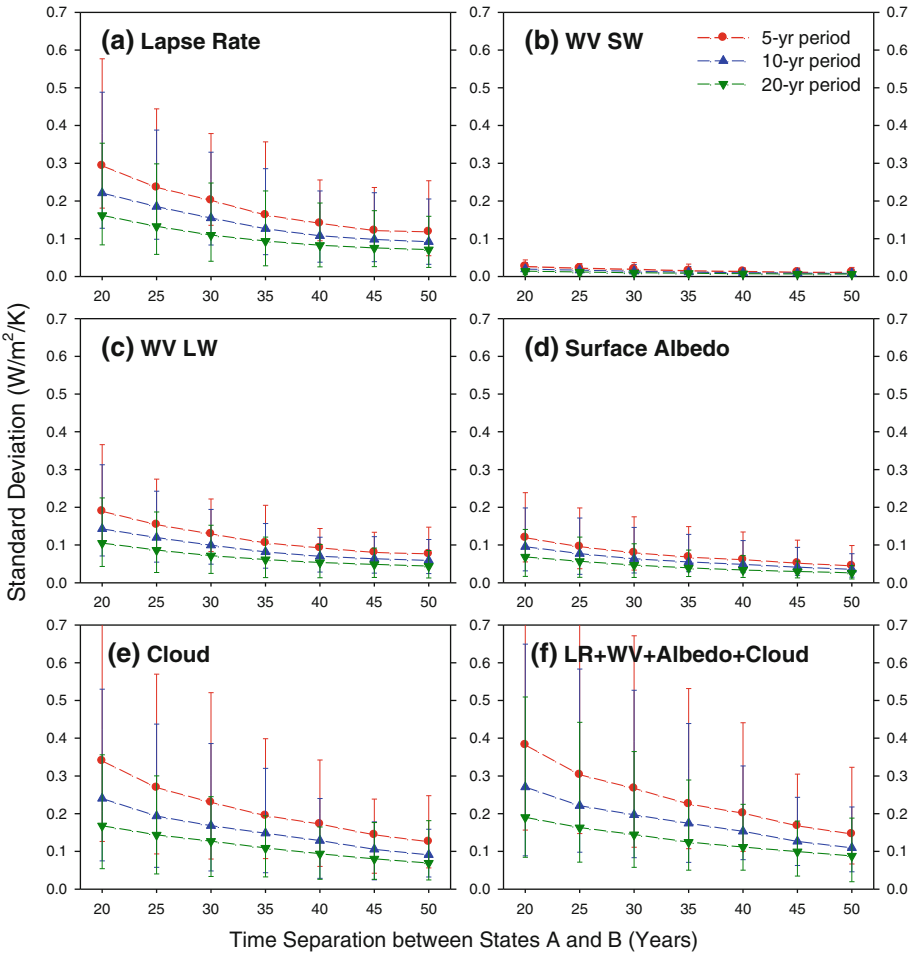

Fig. 4 Variations of standard deviation of the feedback strengths computed from the IPCC AR4 SRES A1B simulations as a function of the time separation between climate states A and B: **a** lapse rate, **b** water vapor (shortwave), **c** water vapor (longwave), **d** surface albedo, **e** cloud, and **f** summation except Planck feedback. *Symbols* and *error bars* denote the average and range of 15 climate models, respectively. *Different symbols* represent different length of the time average used to define climate states

measurements may not be needed if future observing systems have sufficiently accurate absolute calibration.

The temporal variations and intermodel variability of feedback strengths gradually decrease as the climate state B is located far from the climate state A. The extent of decrease is listed in the descending order as follows: cloud, lapse rate, water vapor (longwave component), surface albedo, and water vapor (shortwave component), indicating the differences in temporal variability between feedback processes. For example, weak feedbacks, such as the shortwave component of water vapor feedback, can be accurately quantified from a short period of observations. On the other hand, we need considerably longer satellite observations/model simulations to reduce uncertainties for other feedback processes that are stronger or more variable, for example, cloud feedback

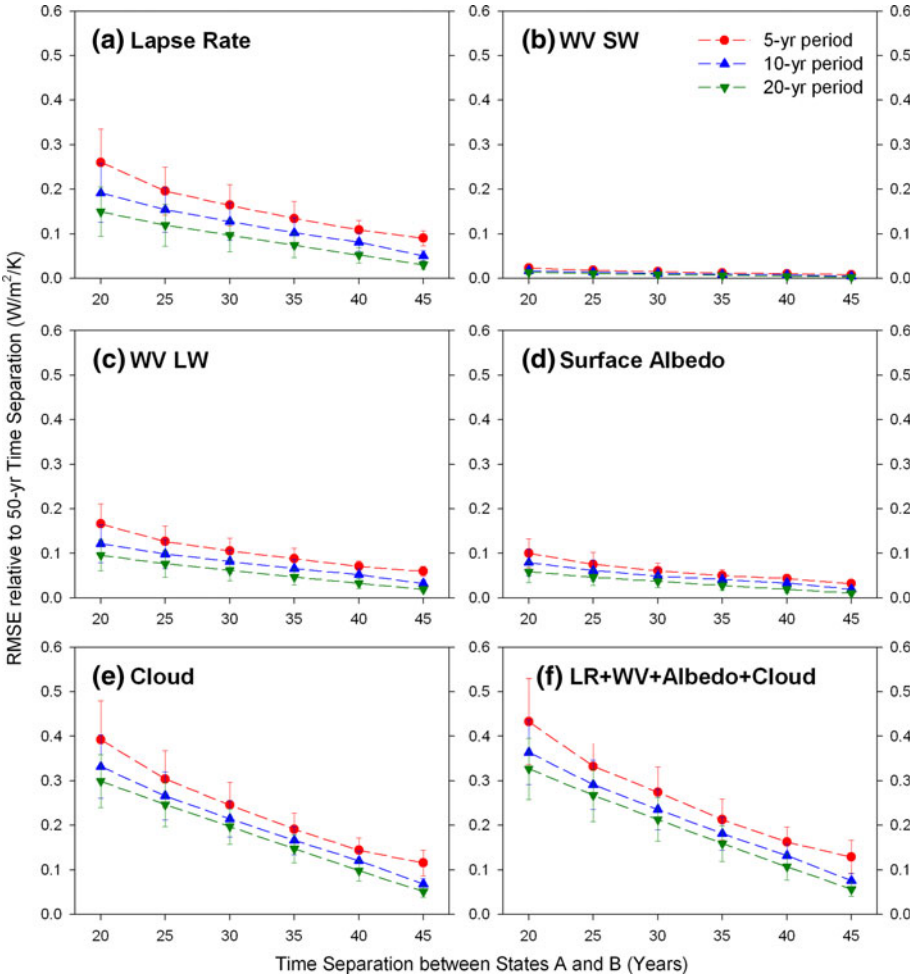

Fig. 5 The root-mean-square-errors of the feedback strengths computed from the IPCC AR4 SRES A1B simulations relative to the 50-year time separation cases: **a** lapse rate, **b** water vapor (shortwave), **c** water vapor (longwave), **d** surface albedo, **e** cloud, and **f** summation except Planck feedback. *Symbols* and *error bars* denote the average and standard deviation of 15 climate models, respectively. *Different symbols* represent different length of the time average used to define climate states

(Senior and Mitchell 2000; Chung et al. 2010b; Dessler 2010). This time dependence of feedback strengths is mainly attributable to the inter-hemispheric difference of temperature change associated with the large thermal inertia of Southern Ocean (Senior and Mitchell 2000).

Finally, we examine the relative accuracy of computed feedback strengths in terms of root-mean-square-error assuming that the 50-year time separation case produces true values. While the use of more long-term model simulations/satellite observations does not substantially improve the accuracy of inferred feedback strengths in the cases of the shortwave component of water vapor feedback and surface albedo feedback, Fig. 5 clearly exhibits a significant reduction in the uncertainty for cloud feedback and the combined feedback with the increase in the time separation between two climate states. These results

suggest that we can keep reducing the uncertainty of cloud feedback and the combined feedback (or climate sensitivity) with the accumulation of satellite observations under the assumption that the satellite measurements are perfect and thus reduce the present inter-model discrepancy of climate sensitivity.

In this study, the time dependence of climate feedbacks has been examined using a radiative kernel approach. However, due to the insufficient record of observations, it may not be practical to derive feedback strengths from observations using a radiative kernel method. Instead, another approach such as regressing radiative fluxes at the top-of-atmosphere with surface temperature can be utilized for observation-based estimation of climate feedbacks (e.g., Dessler and Wong 2009; Dessler 2010). Therefore, better understanding of the time dependence of climate feedbacks may be obtained for shorter time scales by applying the regression approach to both observations and climate model simulations.

Acknowledgments We would like to thank two anonymous reviewers for their constructive and valuable comments which led to an improved version of the manuscript. We also thank Bruce Wielicki and David Young of NASA Langley Research Center for valuable discussion. This research was supported by a grant from the NASA/CLARREO Program and the NOAA Climate Program Office.

References

Allan RP (2006) Variability in clear-sky longwave radiative cooling of the atmosphere. J Geophys Res 111:D22105. doi:10.1029/2006JD007304

Bony S, Dufresne J-L (2005) Marine boundary layer clouds at the heart of tropical cloud feedback uncertainties in climate models. Geophys Res Lett 32:L20806. doi:10.1029/2005GL023851

Bony S et al (2006) How well do we understand and evaluate climate change feedback processes? J Clim 19:3445–3482

Cess RD et al (1990) Intercomparison and interpretation of climate feedback processes in 19 atmospheric general circulation models. J Geophys Res 95(D10):16601–16615

Chung E-S, Yeomans D, Soden BJ (2010a) An assessment of climate feedback processes using satellite observations of clear-sky OLR. Geophys Res Lett 37:L02702. doi:10.1029/2009GL041889

Chung E-S, Soden BJ, Sohn B-J (2010b) Revisiting the determination of climate sensitivity from relationships between surface temperature and radiative fluxes. Geophys Res Lett 37:L10703. doi:10.1029/2010GL043051

Colman R (2003) A comparison of climate feedbacks in general circulation models. Clim Dyn 20:865–873

Colman R, McAvaney B (2009) Climate feedbacks under a very broad range of forcing. Geophys Res Lett 36:L01702. doi:10.1029/2008GL036268

Dessler AE (2010) A determination of the cloud feedback from climate variations over the past decade. Science 330:1523–1527

Dessler AE, Wong S (2009) Estimates of the water vapor climate feedback during El Niño-Southern Oscillation. J Clim 22:6404–6412

Dessler AE, Zhang Z, Yang P (2008) Water-vapor climate feedback inferred from climate fluctuations, 2003–2008. Geophys Res Lett 35:L20704. doi:10.1029/2008GL035333

Hansen J, Lacis A, Rind D, Russell G, Stone P, Fung I, Ruedy R, Lerner J (1984) Climate sensitivity: analysis of feedback mechanisms, in climate processes and climate sensitivity. AGU, Washington, pp 130–163

John VO, Soden BJ (2007) Temperature and humidity biases in global climate models and their impact on climate feedbacks. Geophys Res Lett 34:L18704. doi:10.1029/2007GL030429

Murphy JM (1995) Transient response of the Hadley Centre coupled ocean-atmosphere model to increasing carbon dioxide. Part III: analysis of global-mean response using simple models. J Clim 8:496–514

Murphy DM, Solomon S, Portmann RW, Rosenlof KH, Forster PM, Wong T (2009) An observationally based energy balance for the Earth since 1950. J Geophys Res 114:D17107. doi:10.1029/2009JD012105

National Research Council (2007) Earth science and applications from space: national imperatives for the next decade and beyond. The National Academies Press, Washington

Senior CA, Mitchell JFB (2000) The time-dependence of climate sensitivity. Geophys Res Lett 27:2685–2688

Shell KM, Kiehl JT, Shields CA (2008) Using the radiative kernel technique to calculate climate feedbacks in NCAR's Community Atmospheric Model. J Clim 21:2269–2282

Soden BJ, Held IM (2006) An assessment of climate feedbacks in coupled ocean-atmosphere models. J Clim 19:3354–3360

Soden BJ, Broccoli AJ, Hemler RS (2004) On the use of cloud forcing to estimate cloud feedback. J Clim 17:3661–3665

Soden BJ, Held IM, Colman R, Shell KM, Kiehl JT, Shields CA (2008) Quantifying climate feedbacks using radiative kernels. J Clim 21:3504–3520

Wetherald RT, Manabe S (1988) Cloud feedback processes in a general circulation model. J Atmos Sci 45:1397–1415

Zhang MH, Hack JJ, Kiehl JT, Cess RD (1994) Diagnostic study of climate feedback processes in atmospheric circulation models. J Geophys Res 99:5525–5537